HHS Public Access

Author manuscript

Exp Eye Res. Author manuscript; available in PMC 2021 February 01.

Published in final edited form as:

Exp Eye Res. 2020 February ; 191: 107903. doi:10.1016/j.exer.2019.107903.

In vitro Response and Gene Expression of Human Retinal Müller Cells Treated with Different Anti-VEGF Drugs

Javier Cáceres-del-Carpio, MD[a,1,2,*], **M. Tarek Moustafa, MD FRCS**[a,3,*], **Jaime Toledo-Corral, MD**[a], **Mohamed A. Hamid, MD**[a,3], **Shari R. Atilano, MS**[a], **Kevin Schneider, PhD**[a], **Paula S. Fukuhara, MD**[a], **Rodrigo Donato Costa, MD**[a,4], **J. Lucas Norman, BS**[a], **Deepika Malik, MD**[a,5], **Marilyn Chwa, MS**[a], **David S. Boyer, MD**[b], **G. Astrid Limb, PhD**[c], **M. Cristina Kenney, MD, PhD**[a,d], **Baruch D. Kuppermann, MD, PhD**[a,e]

[a]Gavin Herbert Eye Institute, University of California, Irvine, California, USA

[b]Retina-Vitreous Associates Medical Group, Los Angeles, California, USA

[c]Division of Ocular Biology and Therapeutics, UCL Institute of Ophthalmology, London, UK

[d]Department of Pathology and Laboratory Medicine, University of California, Irvine, California, USA

[e]Department of Biomedical Engineering, University of California, Irvine, USA

[1]Facultad de Medicina Humana Manuel Huaman Guerrero – Universidad Ricardo Palma, Lima, Peru

[2]Ophthalmology Service, Hospital Nacional Edgardo Rebagliati Martins – EsSalud, Lima, Peru

[3]Ophthalmology Department, Minia University, Egypt

[4]Instituto Donato Oftalmologia, Poços de Caldas, MG, Brazil

[5]Laurel Eye Clinic, Brookville, Pennsylvania, USA

1. INTRODUCTION:

In the past decade, anti-vascular endothelial growth factor (VEGF) therapy has become more popular and the standard of care for several retinal diseases including exudative age-related

Address correspondence to: M. Cristina Kenney, MD, PhD, Professor, Ophthalmology, 843 Health Science Road, Hewitt Hall, Room 2028, Gavin Herbert Eye Institute, University of California, Irvine, Irvine, CA 92697 USA, mkenney@uci.edu, Phone: +1-949-824-7603.

*These authors contributed equally to this article.

9.FINANCIAL DISCLOSURE:

All authors have no financial interest to disclose related to this work except the last author, Baruch D. Kuppermann who is a consultant to Alcon, Alimera, Allegro, Allergan, Catalyst, Cell Care, Cell-Cure, Dose, Eyedaptic, Genentech, Glaukos, GSK, J-Cyte, Novartis, Ophthotech, Re-Vana, Regeneron, Santen, ThromboGenics. M. Cristina Kenney; Discovery Eye Foundation is a 501(c)3 that has supported her mitochondrial research. She serves as a Board Member for DEF. The terms of this arrangement have been reviewed and approved by the University of California, Irvine in accordance with its conflict of interest policies. MCK is a consultant to Allergo Ophthalmics.

macular degeneration (AMD) (Brown et al., 2006; Martin et al., 2012; Rosenfeld et al., 2006; Tufail et al., 2010), diabetic macular edema (DME) (Brown et al., 2013; Do et al., 2012; Do et al., 2013; TDRCR, 2015), and macular edema (ME) due to retinal vein occlusion (RVO) (Brown et al., 2010; Brown et al., 2013; Campochiaro et al., 2010; Wu et al., 2008).

Ranibizumab (Lucentis®, Genentech, San Francisco, CA) is a humanized, recombinant, monoclonal antibody fragment. Intended for intraocular use, a 0.5mg/0.05ml dose is approved by the Food and Drug Administration for exudative AMD and ME due to RVO; a 0.3mg/0.05ml dose is approved by the FDA for DME, and diabetic retinopathy (DR). Bevacizumab (Avastin®, Genentech, San Francisco, CA) is a humanized monoclonal human immunoglobulin gamma 1 (IgG1) antibody that selectively binds to circulating VEGF and inhibit its binding to cell surface receptors. A 1.25mg/0.05ml is used off-label in the United States and is commonly used worldwide for exudative AMD, DME and RVO. Aflibercept (Eylea®, Regeneron Pharmaceuticals, Tarrytown, NY) is a recombinant protein receptor decoy composed of two VEGF receptors 1 and 2 fused with the Fc region of human IgG1. Compared to the former two anti-VEGF drugs, it has a higher binding affinity for VEGF and it also binds to VEGF-B and Placental growth factor (PGF). A concentration of 2.0mg/0.05ml is approved by the FDA for wet AMD, DME, ME due to RVO, and DR in patients with DME.

Ziv-aflibercept (Zaltrap®, Sanofi Aventis, Bridgewater, NJ and Regeneron Pharmaceuticals, Tarrytown, NY), also known as VEGF Trap-oncologic, contains 25 mg/ml ziv-aflibercept, however contains higher sucrose concentrations than aflibercept (Eylea), which results in higher osmolality (Bayer, 2014; Group, 2012). Ziv-aflibercept is approved by the FDA for treatment of resistant or progressing metastatic colorectal cancer. However, Mansour et al. (Mansour et al., 2015; Mansour et al., 2017a; Mansour et al., 2017b); de Oliveira Dias et al. (de Oliveira Dias et al., 2015; de Oliveira Dias et al., 2017; de Oliveira Dias et al., 2016); and Chhablani et al., (Chhablani, 2015; Chhablani et al., 2017), among other authors, have published several reports finding good outcomes and no apparent safety issues in a series of patients treated with intravitreal ziv-aflibercept.

Previous studies have shown that anti-VEGF drugs in clinically significant doses do not affect cell viability *in vitro* in a human retinal pigment epithelium (RPE) cell line (ARPE-19) (Luthra et al., 2006; Malik et al., 2014b). Nonetheless, subtle cytotoxic changes in RPE cells, such as decrease in mitochondrial membrane potential, could be observed even at clinical doses for some anti-VEGF drugs (Malik et al., 2014b). Numerous publications have described *in vitro* differential responses to the different anti-VEGF drugs in various retinal cells (Deissler et al., 2012; Klettner et al., 2010; Schnichels et al., 2013).

Müller cells are predominant glial cells in the retina and provide structural and metabolic support to retinal neurons. Several studies have described numerous functions of Müller cells, including regulation of cellular homeostasis and pH, modulation of neurotransmitter recycling, contribution to the blood-retinal barrier by surrounding retinal capillaries with glial processes (Limb et al., 2002; Reichenbach and Bringmann, 2013), acting as light collectors by directing light to photoreceptors (Franze et al., 2007; Reichenbach and

Bringmann, 2013), and secretion and regulation of VEGF and pigment epithelium derived factor (PEDF) (García and Vecino, 2003; Limb et al., 2002; Reichenbach and Bringmann, 2013). Müller cells have also been associated with retinal neuroprotection, wound healing and regeneration (García and Vecino, 2003).

The purpose of this study was to evaluate the *in vitro* response and differences in gene expression of human retinal Müller cells treated with different concentrations of ranibizumab, bevacizumab, aflibercept or ziv-aflibercept. Assays for cell viability, metabolic activity, mitochondrial membrane potential ($\Delta\Psi m$), reactive oxygen species (ROS) and apoptosis were used to evaluate responses to the anti-VEGF drugs. In addition, differences in the expression levels for angiogenesis-related, pro-apoptotic, inflammation and oxidative stress genes were assessed.

2. METHODS:

2.1. Cell culture:

The immortalized human retinal Müller cell line MIO-M1 was obtained from the Department of Cell Biology of the University College, London. Cells and were cultured in Dulbecco's Modified Eagle's Medium (DMEM) with 4.5g/L glucose, glutaGRO (Corning Cellgro, Manassas, VA), and 10% fetal bovine serum (FBS) as reported previously (Hollborn et al., 2011; Limb et al., 2002; Ramírez et al., 2016). It should be noted that the high glucose levels in both control and treated media are higher than that of healthy individuals (normal glucose levels in the body 70 to 130 mg/dL) and may have some influence on the viability of the cultured cells as well as the expression of different genes. However, the MIO-M1 cell line requires higher glucose levels for healthy culture conditions and some reports in the literature show that these high glucose levels in the culture media did not affect the gene expression levels (Matsuzaki et al., 2014). In this study, MIO-M1 cells were plated in either 6-well, 24-well or 96-well plates for 24 hours before treatment and kept under normal culture conditions of 37° C and 5% carbon dioxide.

2.1 Markers for MIO-M1 cell line:

The morphology of cultured MIO-M1 cells was evaluated by phase contrast microscopy and compared to the original study describing the cell line (Limb et al., 2002). Quantitative real-time-PCR (qRT-PCR) was used to measure expression levels of genes known to be markers for human retinal Müller cells and compared to the ARPE-19 cell markers.

Tissue culture: MIO-M1 cells were cultured as described above. The ARPE-19 cells were obtained from ATTCC (Manassas, VA) and cultured in DMEM mixture 1:1 Ham's F-12 medium (Corning–Cellgro, Mediatech, Manassas, VA), with 10% FBS, penicillin F 100 U/ml, streptomycin sulfate 0.1% mg/mL, gentamicin 10 mg/mL, and amphotericin B 2.5 mg/mL. Briefly, MIO-M1 cells and ARPE-19 cells were plated in 6-well plates and cultured for 24 hours.

RNA extraction and cDNA synthesis: RNA was isolated using the RNeasy Mini-Extraction kit (Qiagen, Inc., Valencia, CA). cDNA was synthesized from 100ng of each

RNA sample using the SuperScript-VILO cDNA Synthesis Kit (Invitrogen - Life Technologies, Eugene, OR).

Gene expression analyses: qRT-PCR (QuantiTect Primer Assay, Qiagen, Inc., Valencia, CA) was performed using primers for actin, alpha 2, smooth muscle, aorta (*ACTA2*, Gene ID 59, NM_00114945) and Glial Fibrillary Acidic Protein (*GFAP*, Gene ID 2670, NM_002055) (Limb et al., 2002). Low levels of *CRALBP* can also be found in Müller cells (Burke, 2008; Dunn et al., 1996; Limb et al., 2002; Reichenbach and Bringmann, 2013).

For comparison the levels for three known markers for RPE cells, *BEST1* (Gene ID 7439, NM_004183) (Burke, 2008), *CRALBP* (Gene ID 6017, NM_000326) (Burke, 2008; Dunn et al., 1996) and *KRT18* (Gene ID 3875, NM_000224) (Burke, 2008) (a marker for RPE differentiation) were measured. Each of the marker genes were compared to the housekeeper gene Hydroxymethylbilane Synthase (HMBS, Gene ID 3145, NM_000190, NM_001024382, NM_001258208, NM_001258209). Subsequently, fold differences of the MIO-M1 cells and ARPE-19 cells were calculated. The samples were run in triplicate and the experiment repeated twice.

qRT-PCR was performed using Power SYBR green master mix on a StepOnePlus Q-PCR system (Applied Biosystems - Life Technologies, Eugene, OR). ΔCt values for each marker gene of interest were calculated through normalization to the internal control HMBS. ΔΔCt values were obtained through comparison of MIO-M1 and ARPE-19 ΔCt values. Folds were calculated with the formula $2^{\Delta\Delta Ct}$.

The ARPE-19 cells were assigned a value of 1 for each of the markers (Figure 1A). In the MIO-M1 cells, the genes expression levels of *ACTA2* (3.4-fold, p = 0.0003) and *GFAP* (21.6-fold, p = 0.01) were significantly higher than transcription levels seen in human ARPE-19 cells (1.0-fold). In contrast, the MIO-M1 cells had very low levels for the three known markers for RPE cells, *BEST1* (0.011-fold, p = 0.0001), *CRALBP* (0.16-fold, p = 0.0007) and *KRT18* (0.016-fold, p =0.0001) relative to the ARPE-19 cells (1.0-fold).

Phase contrast microscopy: MIO-M1 cells were plated in 96-well plates and placed in an IncuCyte instrument (Essen Bioscience, Inc, Ann Arbor, MI) for 72 hours. Images were captured at 24 and 72 hours. Figure 1B shows subconfluent monolayer of MIO-M1 cells displaying bipolar morphology, elongated cytoplasmic projections and a granular intracellular profile, similar to that describe by Limb and coworkers (Limb et al., 2002). Figure 1C shows that confluent MIO-M1 cells maintain their spindle shape and granular appearance.

Some MIO-M1 cultures were treated with anti-VEGF drugs for 24 hours and the IncuCyte® Caspase-3/7 Green Apoptosis Assay Reagent probe (Cat. No. 4440, DNA intercalating dye) was added to measure the levels apoptosis. This probe is non-perturbing to cell growth and morphology *in vitro* systems. When apoptosis occurs, this inert probe crosses the cell membrane, is cleaved by activated Caspase 3/7 and becomes fluorescent. The excitation wavelength is 500 nm and the emission wavelength is 530 nm. All analysis was done

utilizing the IncuCyte S3 2019A software (Essen Bioscience, Inc. Ann Arbor, MD). Caspase-3 levels, a late stage of apoptosis, were normalized to nuclear count as measured by Nuclight Live Cell imaging Reagent (Cat. No. 4625).

1.1. Treatments

Cells were treated for 24 hours with either ranibizumab, bevacizumab, aflibercept or ziv-aflibercept in 1x and 2x concentrations. The 1x clinical dose was defined as 0.05ml injected into 4mls vitreous, which equals a concertation of 0.5mg ranibizumab, 1.25mg bevacizumab and 2mg aflibercept. For ziv-aflibercept, for which the commercially available concentration is 25mg/ml, the 1x was the clinical equivalent dose to aflibercept (2.0mg in 0.05ml) injected in 4ml of vitreous. Under tissue culture conditions, the 1x and 2x drug concentrations were equivalent to the clinical doses described above.

1.2. Cytotoxicity assays

2.4.1. Cell viability assay (Trypan blue dye exclusion assay)—MIO-M1 cells were plated in 6-well plates with a concentration of 0.5×10^6 cells per well for 24 hours, and treated for an additional 24 hours with the four drugs in the different concentrations. Cells were harvested and cell viability (CV) was assessed by trypan blue dye exclusion with an automated ViCell cell viability analyzer (Beckman Coulter Inc., Fullerton, CA). This assay is based on the principle that cells with intact membranes can exclude the trypan blue dye while dead cells are permeable and take up the dye. Results were normalized to untreated 100%.

2.4.2. Cellular metabolic activity (MTT assay)—Cells were plated in 96-well plates at 20×10^3 cells per well and treated accordingly as described previously. As per the manufacturer's protocol, 10μl of tetrazolium MTT dye (3-(4,5-dimethylthiazol-2-yl)-2,5-diphenyltetrazolium bromide; Biotium, Hayward, CA) was added to each well; after 1.5 hours incubation in 37°C, 200μl of dimethyl sulfoxide (DMSO) was added to each well. Absorbance signal at 570nm and background absorbance at 630nm were measured using a BioTek ELx808 absorbance plate reader (BioTek, Winooski, VT). Absorbance ratios were normalized to untreated 100%. The MTT assay, which assesses the metabolism of yellow tetrazolium MTT salt into purple formazan crystal by active cells, is quantified by measuring the absorbance and is proportional to the number of viable cells (Mosmann, 1983).

2.4.3. Mitochondrial membrane potential (ΔΨm)—0.1×10^6 cells per well were plated in 24-well plates and treated with anti-VEGF drugs as described previously. The JC-1 detection kit (Biotium Inc., Hayward, CA) was used to assess the ΔΨm. The JC-1 dye (5,5′,6,6′-tetrachloro-1,1′,3,3′-tetraethyl-benzimidazolyl-carbocyanineiodide) is a cationic dye that accumulates in the mitochondrial membranes of healthy cells resulting in red fluorescence. Stressed or damaged cells show reduced ΔΨm and accumulates the dye in the cytosol instead of the mitochondria, resulting in green fluorescence. To obtain the changes in ΔΨm, the ratio of red to green fluorescence was calculated. Cells were exposed to a 1:100 solution of the stock JC-1 dye in phenol-red free medium and incubated in 37°C for 15 minutes. A Biotek Synergy HT plate reader (Biotek, Winooski, VT) was used to measure the fluorescent signals, set to detect green (excitation (EX) 485nm, emission (EM) 535nm) and

red (EX 550nm, EM 600nm) emissions; and red to green ratios were calculated. Results were normalized to untreated 100%.

2.4.4. Reactive oxygen species (ROS) production—Cells were plated in 24-well plates and treated as described previously. ROS production was assessed using the fluorescent dye 2',7'-dichlorodihydrofluorescein diacetate (H2DCF-DA; Molecular Probes–Life Technologies, Eugene, OR). This assay detects hydrogen peroxide, hydroxyl radicals, and peroxynitrite anions. Cells were exposed to 10μM of H2DCF-DA in PBS and incubated for 30 minutes at 37°C. The fluorescent signal was measured using the Biotek Synergy HT plate reader (Biotek, Winooski, VT) with EX filter in 490nm and EM filter in 520nm. Results were normalized to untreated 100%.

2.4.5. YO-PRO-1 apoptosis assay—Cells were plated in 24-well plates and treated accordingly. YO-PRO-1 iodide (Molecular Probes-Life Technologies, Eugene, OR) is a nucleic acid dye that enters cells in early stages of apoptosis without interfering in cell viability (Glisic-Milosavljevic et al., 2005; Idziorek et al., 1995). Apoptotic cells show green fluorescence. Cells were exposed to 1μM of YO-PRO-1 dye in phenol-red free medium and incubated for 20 minutes over ice. A Biotek synergy HT plate reader (Biotek, Winooski, VT) was used to measure fluorescence with EX 491nm and EM 509nm. Results were normalized to untreated 100%.

2.5 Gene expression

Cells were plated in 6-well plates and treated with the anti-VEGF drugs as described previously. RNA was isolated using the RNeasy Mini-Extraction kit. cDNA was synthesized from 100ng of each RNA sample using the SuperScript-VILO cDNA Synthesis Kit (Invitrogen-Life Technologies, Eugene, OR). Quantitative polymerase chain reaction (Q-PCR) was performed using primers (QuantiTect Primer Assay, Qiagen, Inc., Valencia, CA) for the following genes (Table 1). The angiogenesis-related genes included vascular endothelial growth factor A (*VEGFA*), placental growth factor (*PGF* or *PlGF*) and hypoxia inducible factor 1 alpha (*HIF1A*), key regulatory genes responsible for neovascularization in many disease processes. Apoptosis is a common feature of the retinal degeneration occurring in AMD, and two representative pro-apoptotic genes, B-cell lymphoma 2 like 13 (*BCL2L13*) and BCL2-associated X protein (*BAX*), were analyzed in our cultures. The genes representing the inflammation pathway were interleukin 1 beta (*IL1β*) and interleukin 18 (*IL18*), which are increased with aging, expressed after Caspase-1 activation and accumulate in chronic retinal degenerations, including AMD (Campbell et al., 2014; Franceschi and Campisi, 2014; Goldberg and Dixit, 2015). The anti-oxidative enzyme genes measured were glutathione peroxidase 3 (*GPX3*) and superoxide dismutase 2 (*SOD2*), both of which are important for removal of hydrogen peroxide and superoxide from retinal cells, respectively. Knockdown of SOD2 within the RPE cells results in a mouse model with key features of AMD (Biswal et al., 2016).

Quantitative real-time - polymerase chain reactions (qRT-PCR) were performed using Power SYBR green master mix on a StepOnePlus Q-PCR system. Housekeeper genes with comparable amplification efficiencies were chosen: Aminolevulinic Acid Synthase variant 1

(*ALAS1*, for *GPX*, *PGF*, *HIF1α* and *IL1β* genes), hypoxanthine-guanine phosphoribosyltransferase 1 (*HPRT 1*, for *SOD2*, *VEGFA*, *IL18* and *BAX* genes) and hydroxymethylbilane synthase (*HMBS*, for *BCL2L13* gene). For the gene expression, qRT-PCR was run in triplicate; ΔΔCt values were obtained and folds were calculated with the formula $2^{\Delta\Delta Ct}$. The gene expression levels of untreated controls were assigned a value of 1. Fold values >1 indicate gene upregulation and fold values <1 indicate gene downregulation.

2.6 Statistical analyses

Data were analyzed with unpaired t-test using the GraphPad Prism version 5.00 for Windows (GraphPad Software, San Diego, CA). Error bars in the graphs represent standard error of mean (SEM). For CV, MTT, ΔΨm, ROS and apoptosis assays: Experiments were run in quadruplicates and repeated three times; all the results were normalized to the untreated control as 100%. Values of $p < 0.05$ (*) statistically significant; $p < 0.01$ (**) very significant; $p < 0.001$ (***) extremely significant.

3 RESULTS:

3.1. Dye exclusion cell viability (CV)

Human Müller cells exposed to ranibizumab, bevacizumab, aflibercept or ziv-aflibercept showed no significant difference in mean percentage CV (CV%) in any of the drugs and any of the concentrations used compared to untreated cultures. Ranibizumab showed CV% of 95.84 ± 0.50, 95.50 ± 0.50 and 95.20 ± 0.39; and bevacizumab showed 95.51 ± 0.31, 95.06 ± 0.48 and 96.06 ± 0.39 of CV% for untreated, 1x and 2x, respectively (Figures 2A, 2B). Aflibercept showed 96.23 ± 0.57 for untreated, 95.43 ± 0.57 for 1x and 95.80 ± 0.37 for 2x dose (Figure 2C). CV% of 95.23 ± 0.68, 96.18 ± 0.65 and 94.60 ± 0.52 were observed for ziv-aflibercept untreated, 1x and 2x respectively (Figure 2D).

3.2. MTT assay

Retinal Müller cells exposed to all the drugs in both concentrations, showed significantly lower relative cell growth (lower tetrazolium MTT salt metabolism) when compared to untreated 100%. Ranibizumab showed 85.65 ± 1.15 and 88.17± 1.94, with $p < 0.0001$ and $p = 0.0004$ for 1x and 2x, respectively (Figure 3A). Bevacizumab showed 83.57 ± 1.69 ($p < 0.0001$) and 87.92 ± 2.48 ($p = 0.0012$) for 1x and 2x doses, respectively (Figure 3B). Aflibercept presented 81.72 ± 1.51 ($p < 0.0001$) for 1x, and 85.44 ± 2.63 ($p = 0.0002$) for 2x doses (Figure 3C). Ziv-aflibercept showed 84.89 ± 1.47 for 1x and 81.65 ± 1.66 for 2x, with $p < 0.0001$ for both concentrations (Figure 3D).

3.3. Mitochondrial membrane potential (ΔΨm)

MIO-M1 cells exposed to ranibizumab showed no significant difference in mitochondrial membrane potentials for 1x dose (99.33 ± 2.31) and 2x dose (97.34 ± 2.31) compared to untreated cultures normalized to 100% (Figure 4A). Cells exposed to bevacizumab (1x dose) (93.87 ± 3.72) showed no significant difference in ΔΨm compared to untreated. However, the 2x dose (85.74 ± 4.49) was significantly lower than untreated controls ($p = 0.03$) (Figure 4B). For aflibercept, the 1x dose showed mitochondrial membrane potential of 85.28 ± 2.87 ($p = 0.0008$) and the 2x dose demonstrated 85.02 ± 3.80 ($p = 0.0031$), respectively, when

compared to untreated (Figure 4C). Ziv-aflibercept showed a decrease in ΔΨm for 1x dose 85.39 ± 3.47 (p = 0.0016) and 2x with 86.01 ± 4.62, (p = 0.0116), respectively when compared to untreated (Figure 4D).

3.4. ROS

Retinal Müller cells exposed to ranibizumab showed increased levels of ROS at the 1x (136.90 ± 4.67) and 2x (139.83 ± 6.53) doses with p < 0.0001 for both when compared to untreated (Figure 5A). Higher ROS levels were also found for bevacizumab at the 1x (124.13 ± 5.47, p = 0.0017) and 2x (133.92 ± 8.10, p = 0.0011) doses as compared to untreated (Figure 5B). Aflibercept at the 1x dose showed ROS levels of 129.62 ± 3.08 whereas the 2x dose showed 130.27 ± 4.58, with p < 0.001 for both compared to untreated (Figure 5C). Higher levels for ROS were also found for Ziv-aflibercept at the 1x (140.27 ± 9.92, p = 0.0001) and 2x (144.28 ± 12.02, p = 0.0004) doses when compared to untreated (Figure 5D).

3.5. YO-PRO-1 apoptosis

MIO-M1 cells showed higher levels of early apoptosis compared to untreated cultures when exposed to all the drugs in both concentrations. Ranibizumab 1x dose showed 133.48 ± 8.35 (p = 0.0107), ranibizumab 2x dose 141.35 ± 7.40 (p = 0.0039), bevacizumab 1x dose 133.26 ± 7.95 (p = 0.0037), bevacizumab 2x dose 140.21 ± 7.68 (p = 0.0005), aflibercept 1x dose 169.17 ± 12.23 (p = 0.0001), aflibercept 2x dose 179.00 ± 11.23 (p < 0.0001), ziv-aflibercept 1x dose 154.72 ± 13.19 (p = 0.0062), and ziv-aflibercept 2x dose 171.16 ± 17.36 (p = 0.0039) when compared to untreated cultures normalized to 100% (Figures 6A – 6D). During the IncuCyte studies, after a 24-hour incubation period with anti-VEGF drugs, the probe for Caspase-3 levels was added to the cultures and activation levels were measured. There was no significant change in the caspase 3 levels in the anti-VEGF drugs (data not shown).

3.6. Gene expression (Tables 2A–2D)

VEGFA was found to be significantly downregulated in both concentrations of all the drugs studied except in ziv-aflibercept 2x dose. *PGF* was found to be significantly upregulated in bevacizumab 1x and aflibercept 1x and 2x; and significantly downregulated in ziv-aflibercept 1x and 2x. No significant differences were found in the *HIF1A* levels in any of the drugs studied. The *BAX* expression levels were not found to be significantly different except at the 1x bevacizumab and ziv-aflibercept 1x and 2x doses. The *BCL2L13* expression levels were significantly upregulated in 1x ranibizumab, 1x and 2x bevacizumab, 1x and 2x aflibercept, and 1x ziv-aflibercept.

IL1β was significantly upregulated ranibizumab 1x and 2x and bevacizumab 1x, but was not significantly changed in bevacizumab 2x or any concentration of aflibercept and ziv-aflibercept. *IL18* was significantly upregulated in ranibizumab 1x and ziv-aflibercept 1x and 2x. A significant downregulation for *SOD2* expression was found in both concentrations in all the drugs studied. A significant difference was seen in the upregulation for *GPX3* levels at the 1x and 2x concentrations of ranibizumab, bevacizumab and aflibercept. No significant differences were found for *GPX3* gene in any of the ziv-aflibercept concentrations.

4. DISCUSSION:

Anti-VEGF therapy is the mainstay for treatment of many retinal diseases. Previous clinical studies have confirmed its safety and effectiveness in treating AMD (Brown et al., 2006; Martin et al., 2012; Rosenfeld et al., 2006; Tufail et al., 2010), DME (Do et al., 2012; Do et al., 2013; TDRCR, 2015) and RVO (Brown et al., 2010; Brown et al., 2013; Campochiaro et al., 2010; Wu et al., 2008). However, they have the potential to cause increases in the size of geographic atrophy in patients with AMD (Grunwald et al., 2014; Martin et al., 2012) and possibly worsening of macular ischemia in DME (Manousaridis and Talks, 2012).

In this investigation, we tested commercially available anti-VEGF drugs on an immortalized cell line of human retinal Müller cells (MIO-M1). Müller cells have very important functions including maintenance of the blood retinal barrier (Constable and Lawrenson, 2009; Sarthy and Lam, 1978); secretion and regulation of pigment epithelium derived factor (*PEDF*) and *VEGF* (García and Vecino, 2003; Limb et al., 2002; Reichenbach and Bringmann, 2013) along with neuroprotection during wound healing and regeneration (García and Vecino, 2003). Even after initial improvement of retinal anatomy and visual acuity, some subjects receiving long-term administration of anti-VEGF injections develop geographic atrophy.

In a study by Matsuda et al., when they exposed the MIO-M1 cell line to bevacizumab 0.25 mg/ml or 0.5 mg/ml and evaluated cell viability (dye exclusion and MTT assays), levels of apoptosis (Caspase-3 gene expression) and autophagy, they found no significant differences in cell viabilities as measured by trypan blue assay at any bevacizumab concentration or length of exposure, very similar to our results. When mitochondrial metabolic rates were measured with the MTT assay, they found higher levels at 24 hours compared to the 12-hours treatment (Matsuda et al., 2017). In contrast, our MIO-M1 cultures, which were cultured 24 hours, showed lowered MTT metabolism for all drugs studied, including the bevacizumab.

With respect to apoptosis, this group used two bevacizumab concentrations (25 and 50 mg/ml), and reported the increased gene expression of Caspase-3 at the 12-hour timepoint, but not at 24 hours and suggested that cells may have adapted to the bevacizumab through increased metabolic activity (Matsuda et al., 2017). Romano and co-workers showed some TUNEL staining and apoptosis in the retinal ganglion cells of rat eyes 48 hours after a single injection of bevacizumab, where the staining significantly increased with multiple injections (Romano et al., 2012). In our study, using 25 mg/ml bevacizumab, we found increased ROS production and early apoptosis as measured by higher YO-PRO-1 levels. The $\Delta\Psi m$ (another marker for early apoptosis) decreased in bevacizumab at the 2x dose, and both concentrations of aflibercept and ziv-aflibercept. However, cell viability, as measured by trypan blue assay, was not decreased at the 24-hour time point for any of the anti-VEGF drugs. This was not totally surprising because the trypan blue assay measures viable cells that have intact cell membrane that exclude dyes, indicating when the cells are dead or viable. Caspase-3 levels measured in the MIO-M1 cells after 24 hours incubation with anti-VEGF drugs were not significantly elevated compared to the untreated cultures (data not shown). This suggests that the stressed MIO-M1 cells may show signs of early apoptosis

(higher YO-PRO-1 and lower ΔΨm) but have not reached the later stages of apoptosis (Caspase-3 activation) so their cell membranes are still intact and cell viability is normal. Similar results were shown in the ARPE-19 cells, whereby the cell viability was unchanged after a 24-hour exposure to the anti-VEGF drugs however, the ΔΨm was decreased (Malik et al., 2014a). Perhaps if we had evaluated the MIO-M1 cultures at later time points and/or used higher concentrations of the anti-VEGF drugs, we may have seen loss of cell viability in addition to the apoptosis changes.

In this investigation, we also studied the effects of these anti-VEGF drugs on cell metabolism, which was first described by Mossman (Mosmann, 1983). The Müller cells showed decreased levels of metabolism/viability at the 1x and 2x doses of the four drugs. These results are consistent with the work on primary porcine RPE cells (Klettner et al., 2010), where bevacizumab and ranibizumab decreased the cellular metabolism/viability. Guo et al., showed no change in the number of viable rat retinal Müller glial cells (RMGCs) after 72 hours of treatment with bevacizumab as determined using both the trypan blue dye exclusion and MTT colorimetric assays (Guo et al., 2010). A study by Spitzer et al. (Spitzer et al., 2007), initially tested the effects of bevacizumab on different ocular cells (human RPE, rat retinal ganglion cells (RGC5), and pig choroidal endothelial cells (CEC), and discovered decreased incorporation of 5'-bromo-2'-deoxyuridine (BrdU) cell after 2 days.

In our gene expression studies, we found decreased expression levels of *VEGFA* in all drug concentrations expect 2x ziv-aflibercept. *PGF* levels were not changed in ranibizumab treated cells but were overexpressed in the bevacizumab and aflibercept treated MIO-M1 cells. In contrast, the *PGF* levels were downregulated in ziv-aflibercept treated cultures. There was no change in the *HIF1A* gene expression level in any of the anti-VEGF treated cultures. Our results are consistent with the clinical studies by Zehetner et al., who measured the PGF and VEGFA levels in blood samples of patients with wet AMD treated with intravitreal aflibercept, ranibizumab or bevacizumab and demonstrated that the aflibercept treated patients had decreased plasma VEGFA levels and increased PGF levels (Zehetner et al., 2015). In contrast, the ranibizumab and bevacizumab treated subjects showed decreased levels of both VEGFA and PGF.

The MIO-M1 cells responded differently when treated with ziv-aflibercept compared to treatments with the other anti-VEGF drugs. For example, after treatment with 1x and 2x ziv-aflibercept, the PGF levels decreased while the levels increased with aflibercept and bevacizumab treatment or remained unchanged with ranibizumab treatment. Both aflibercept and ziv-aflibercept have the same active drug, which is a soluble decor receptor that binds to VEGFA, VEGFB and PLGF with greater affinity than their natural receptors, thereby inhibiting the formation of new blood vessels. However, aflibercept was formulated for ocular use, while ziv-aflibercept was formulated for intravenous application in cancer patients (Singh et al., 2017). The osmolarity of ziv-aflibercept is between 815–820mOsm, which can be tolerated when introduced into the blood stream, while aflibercept's osmolarity is between 250–260 mOsm. This level could be less toxic when placed into the relatively small volume of the vitreous chamber. In cultures of ARPE-19 cells treated with anti-VEGF drugs, the osmolality of 10x ziv-aflibercept was 418 mOsm while aflibercept was 317 mOsm (Malik et al., 2014b). Hollborn et al. reported that RPE cells grown in hyperosmotic

media showed altered gene transcription of VEGF, as well as aquaporin water channel genes (Hollborn et al., 2011). It may be that the higher mOsm environmental changes the effective binding capacity of ziv-aflibercept resulting in a different regulation of PGF and VEGFA gene expressions compared to the aflibercept drug.

There were also consistent differences in gene expression levels of *PGF, BAX, BCL2L13, IL18* and *GPX3* observed in the aflibercept versus ziv-aflibercept treated cultures. Again, this may be due to the pharmacological alterations of the ziv-aflibercept formulation of higher sucrose (Group, 2012) and osmolality values compared to aflibercept (Bayer, 2014; Group, 2012; Malik et al., 2014b). The parent pharmaceutical company has consistently warned that the ziv-aflibercept formulation is not compatible with intraocular use. Our *in vitro* findings support that the cellular responses to aflibercept and ziv-aflibercept treatments are different and therefore may not be considered to be inter-changeable drugs.

The overexpression levels of the *BCL2L13*, a pro-apoptotic gene, in cultures treated with anti-VEGF drugs are consistent with our finding of increased apoptosis. In ranibizumab-treated MIO-M1 cells, the pro-inflammatory genes (*IL1β* and *IL18*) were also overexpressed compared to untreated cells. This finding coincides with Golan and coworkers who demonstrated that in hypoxic conditions, the ranibizumab or bevacizumab treated human ARPE-19 and umbilical vein (EA.hy926) also showed altered expression of pro-inflammatory genes (Golan et al., 2014).

A limitation to our study was the use of our transformed cell lines (MIO-M1) to address retinal biology due to the varying nature of these cultures from the non-transformed retinal cells. Using array analyses, the gene expression between transformed and native cell lines can be different based in external factors and stimulation (Tian et al., 2005). Therefore, the results obtained from our *in vitro* cell culture studies are valuable, but additional studies using primary Müller cells isolated from chick (Rios et al., 2019), mouse (Ozawa et al., 2019) or rat retinas (Pereiro et al., 2018) are required and will be the focus of future studies.

5. CONCLUSIONS:

In our MIO-M1 cultures, the anti-VEGF drugs caused decreased metabolism, viability and mitochondrial membrane potential, along with increased ROS and apoptosis levels. The anti-VEGF treated cultures demonstrated altered gene expression levels in antioxidant, pro-apoptotic and pro-inflammatory pathways. These findings indicate that in MIO-M1 cells *in vitro*, the anti-VEGF drugs can mediate expression of non-angiogenesis pathways genes and may contribute to the cytotoxicity associated with chronic anti-VEGF injections.

ACKNOWLEDGMENTS:

We wish to thank Kunal Thaker, BS; Tej Patel, BS; and Carolina Yañez, BS; for their excellent assistance with tissue culture.

8. SUPPORTED BY:

The Discovery Eye Foundation, Iris and B. Gerald Cantor Foundation, Henry L. Guenther Foundation, Polly and Michael Smith, and Max Factor Foundation. Research was supported in part by an unrestricted grant from RPB

(Research to Prevent Blindness) to University of California Irvine. Part of this work was presented in the ARVO meeting in Seattle, 2016 and another part at the ASRS meeting, San Francisco, 2016.

6.: APPENDICES:

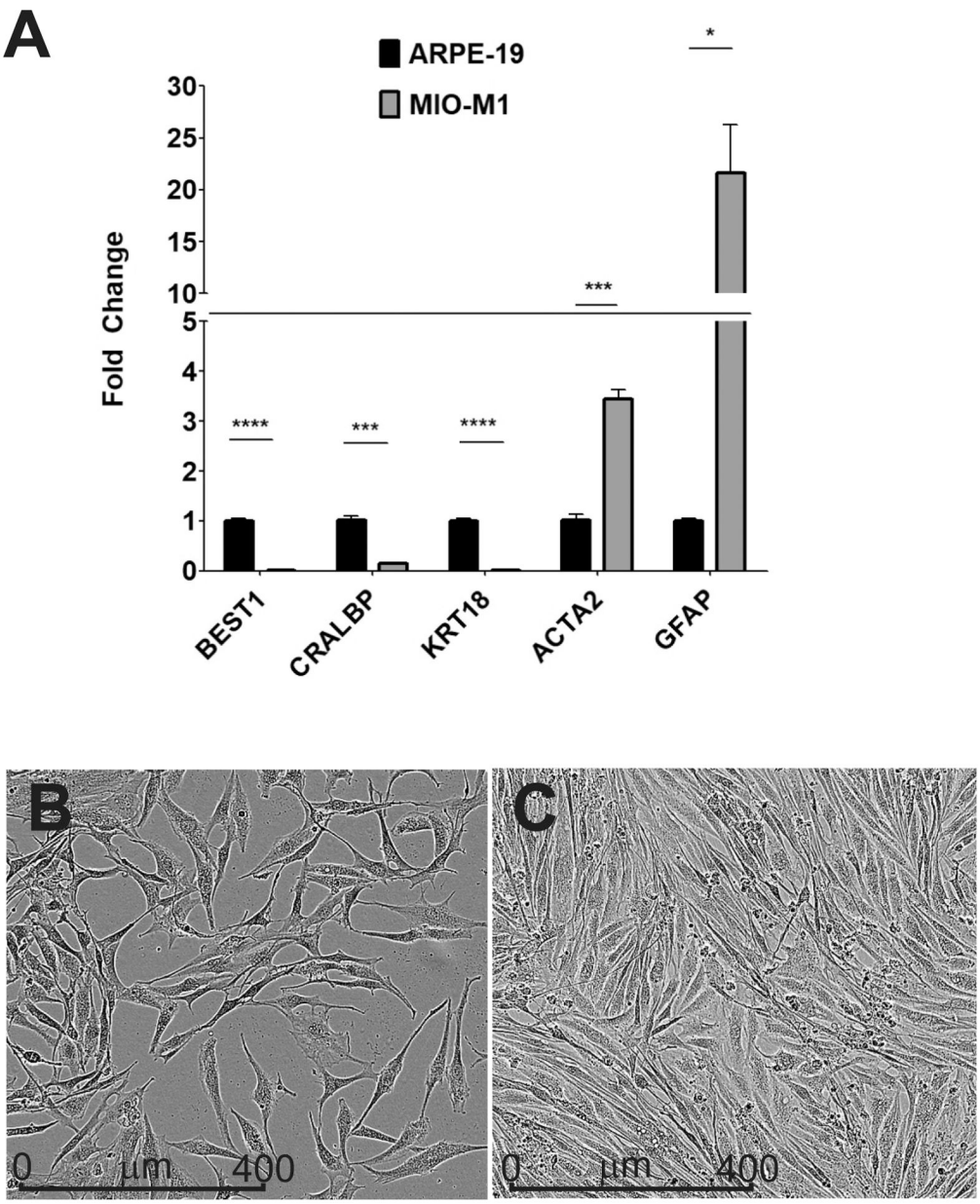

Figure 1.

(**A**) Gene expression levels for Müller cell markers to validate the MIO-M1 cell line. The MIO-M1 and ARPE-19 cells were analyzed by qRTPCR. ARPE-19 samples were assigned a value of 1 for each of the markers. Genes expression levels of the *ACTA2* ($p = 0.0003$) and the *GFAP* ($p = 0.01$) were significantly higher in MIO-M1 cells compared to ARPE-19 cells. MIO-M1 cells had very low levels for the three known ARPE-19 markers (*BEST1*, $p = 0.0.0001$; *CRALBP*, $p = 0.0007$; and *KRT18*, $p = 0.0001$). (**B**) Subconfluent monolayer of MIO-M1 cells shows bipolar extensions, elongated cytoplasmic projections and a granular intracellular profile. (**C**) Confluent monolayer of MIO-M1 cells show MIO-M1 cells maintain their spindle shape and granular appearance.

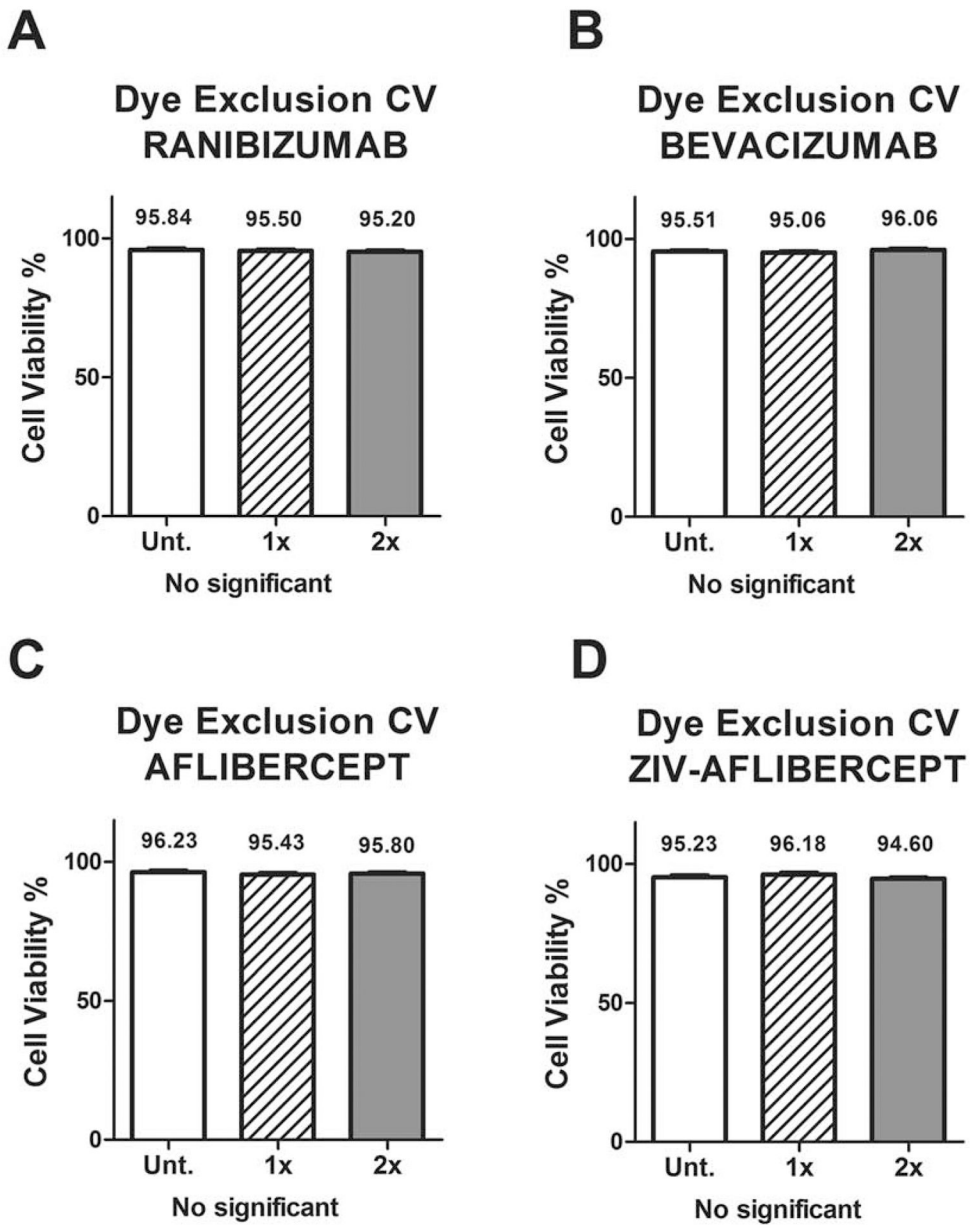

Figure 2.

Cell viability (CV) percentage differences measured by the Trypan blue dye exclusion assay shows no differences between untreated and the tested anti-VEGF treated MIO-M1 cell cultures in the 2 dosage concentrations.

Each group (untreated, 1x and 2x) was plated in duplicate and repeated 3 times.

All p values were greater than 0.05 showing non-statistical significance.

1x: equivalent to the clinical doses of anti-VEGF (0.05ml injected in 4ml of vitreous).

2x: equivalent to double the clinical dose of anti-VEGF.

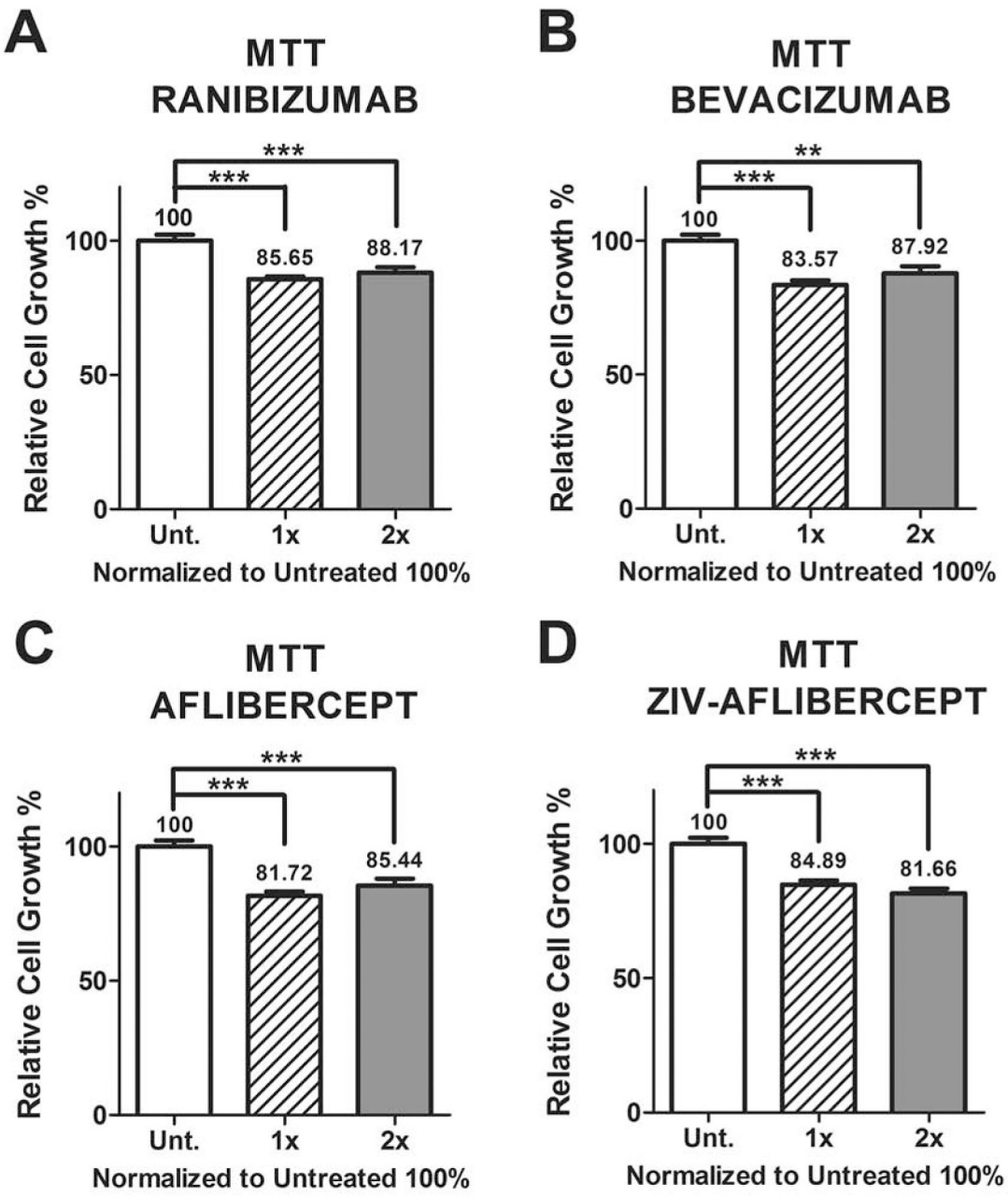

Figure 3.

Cellular metabolic activity was measured by the MTT assay and shows the relative cell growth percentage differences between untreated and anti-VEGF treated MIO-M1 cells with the different concentration dosages.

Each group (untreated, 1x and 2x) was plated in duplicate and repeated 3 times.

*: p value < 0.05; **: p value < 0.01; ***: p value < 0.001; values with non-statistical significance (p > 0.05) have no * signaling.

Control samples assigned a value of 100%.

1x: equivalent to the clinical doses of anti-VEGF (0.05ml injected in 4ml of vitreous).

2x: equivalent to double the clinical dose of anti-VEGF.

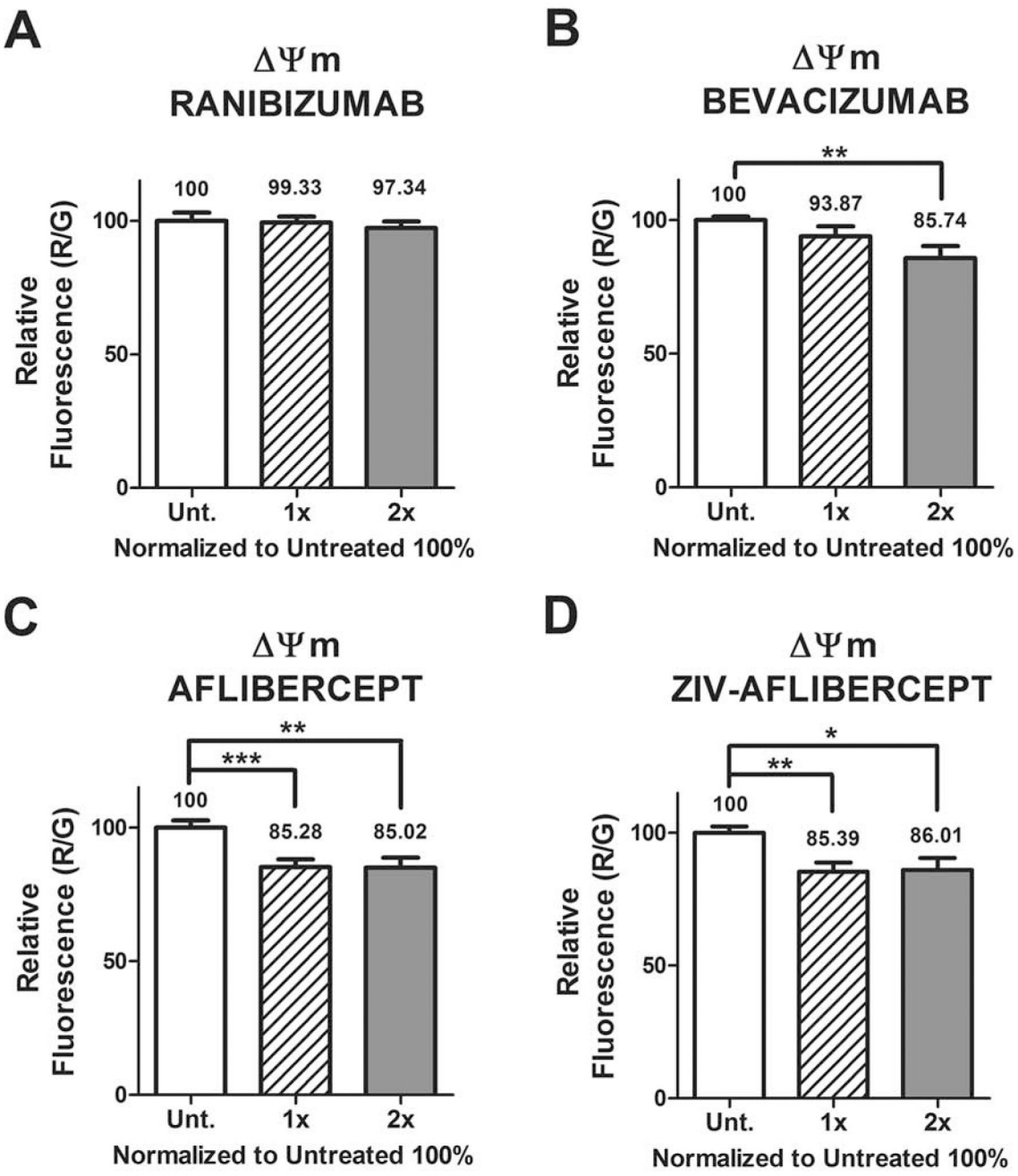

Figure 4.

The mitochondrial membrane potential (ΔΨm) assay shows a decrease in relative fluorescence anti-VEGF treated MIO-M1 cells compared to untreated cultures, in all except with 1 anti-VEGF treatment.

Each group (untreated, 1x and 2x) was plated in duplicate and repeated 3 times.

*: p value < 0.05; **: p value < 0.01; ***: p value < 0.001; values with non-statistical significance (p > 0.05) have no * signaling.

Control samples assigned a value of 100%.

1x: equivalent to the clinical doses of anti-VEGF (0.05ml injected in 4ml of vitreous).

2x: equivalent to double the clinical dose of anti-VEGF.

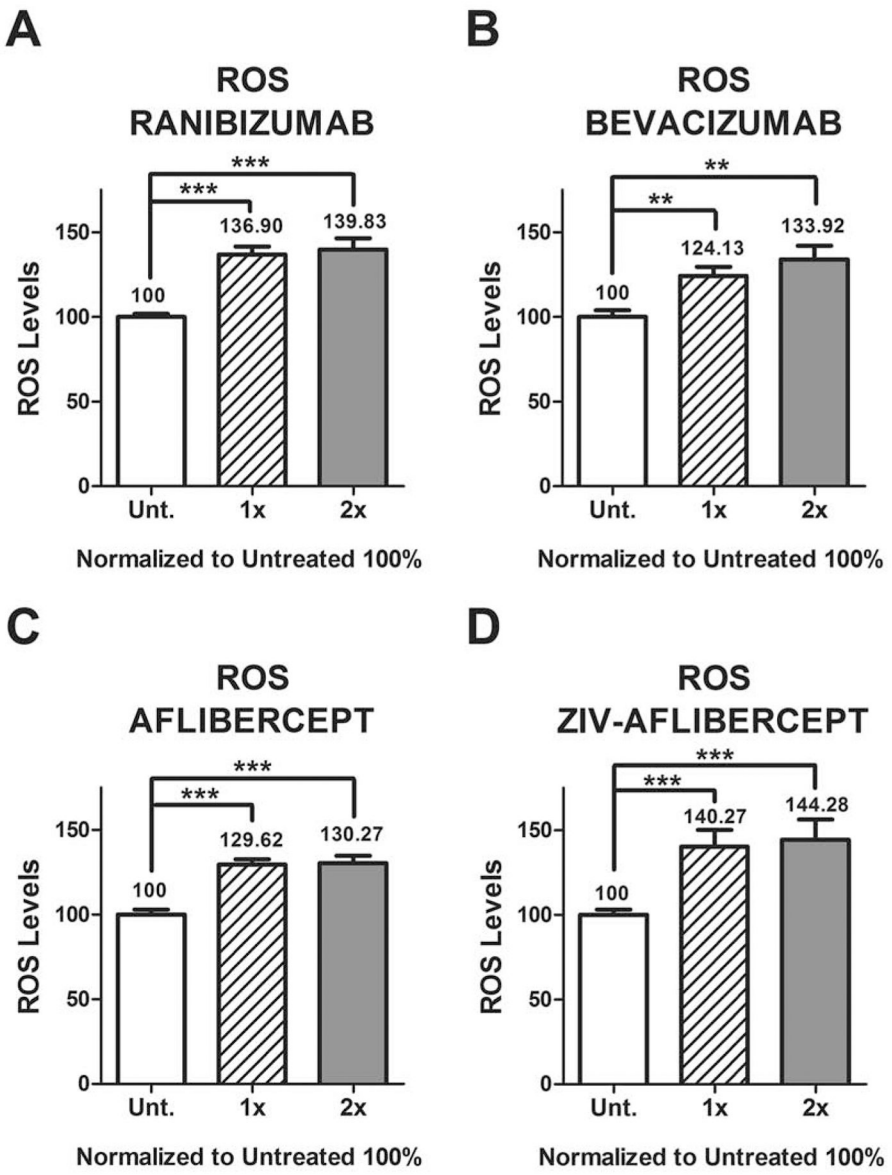

Figure 5.

The levels of ROS production increased in anti-VEGF treated MIO-M1 cells compared to untreated cultures, with the different concentration dosages.

Each group (untreated, 1x and 2x) was plated in duplicate and repeated 3 times.

*: p value < 0.05; **: p value < 0.01; ***: p value < 0.001; values with non-statistical significance (p > 0.05) have no * signaling.

Control samples assigned a value of 100%.

1x: equivalent to the clinical doses of anti-VEGF (0.05ml injected in 4ml of vitreous).

2x: equivalent to double the clinical dose of anti-VEGF.

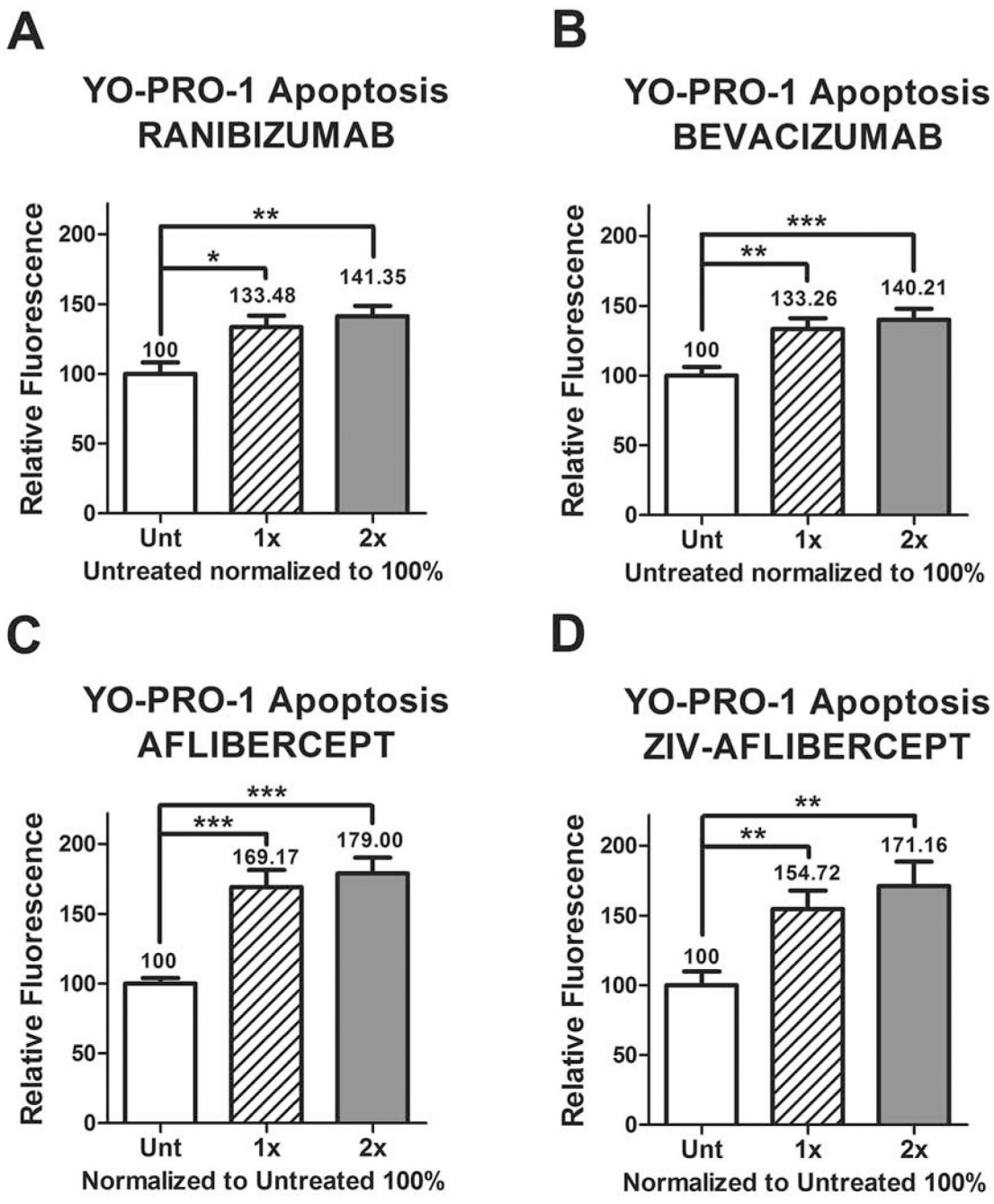

Figure 6.

The YO-PRO-1 apoptosis assay shows increased relative fluorescence levels in the anti-VEGF treated MIO-M1 cells compared to untreated, with the different concentration dosages.

Each group (untreated, 1x and 2x) was plated in duplicate and repeated 3 times.

*: p value < 0.05; **: p value < 0.01; ***: p value < 0.001; values with non-statistical significance (p > 0.05) have no * signaling.

Control samples assigned a value of 100%.

1x: equivalent to the clinical doses of anti-VEGF (0.05ml injected in 4ml of vitreous).

2x: equivalent to double the clinical dose of anti-VEGF.

10. REFERENCES

Bayer, 2014 Eylea™/ VEGF Trap-Onc: Ophthalmic vs Systemic Formulations. Bayer HealthCare.

Biswal MR, Ildefonso CJ, Mao H, Seo SJ, Wang Z, Li H, Le YZ, Lewin AS, 2016 Conditional Induction of Oxidative Stress in RPE: A Mouse Model of Progressive Retinal Degeneration. Advances in experimental medicine and biology 854, 31–37. [PubMed: 26427390]

Brown DM, Campochiaro PA, Singh RP, Li Z, Gray S, Saroj N, Rundle AC, Rubio RG, Murahashi WY, 2010 Ranibizumab for Macular Edema following Central Retinal Vein Occlusion: Six-Month Primary End Point Results of a Phase III Study. Ophthalmology 117, 1124–1133.e1121. [PubMed: 20381871]

Brown DM, Heier JS, Clark WL, Boyer DS, Vitti R, Berliner AJ, Zeitz O, Sandbrink R, Zhu X, Haller JA, 2013 Intravitreal Aflibercept Injection for Macular Edema Secondary to Central Retinal Vein Occlusion: 1-Year Results From the Phase 3 COPERNICUS Study. American journal of ophthalmology 155, 429–437.e427. [PubMed: 23218699]

Brown DM, Kaiser PK, Michels M, Soubrane G, Heier JS, Kim RY, Sy JP, Schneider S, 2006 Ranibizumab versus Verteporfin for Neovascular Age-Related Macular Degeneration. New England Journal of Medicine 355, 1432–1444. [PubMed: 17021319]

Burke JM, 2008 Epithelial phenotype and the RPE: Is the answer blowing in the Wnt? Progress in Retinal and Eye Research 27, 579–595. [PubMed: 18775790]

Campbell M, Doyle SL, Ozaki E, Kenna PF, Kiang AS, Humphries MM, Humphries P, 2014 An overview of the involvement of interleukin-18 in degenerative retinopathies. Advances in experimental medicine and biology 801, 409–415. [PubMed: 24664725]

Campochiaro PA, Heier JS, Feiner L, Gray S, Saroj N, Rundle AC, Murahashi WY, Rubio RG, 2010 Ranibizumab for Macular Edema following Branch Retinal Vein Occlusion: Six-Month Primary End Point Results of a Phase III Study. Ophthalmology 117, 1102–1112.e1101. [PubMed: 20398941]

Chhablani J, 2015 Intravitreal ziv-aflibercept for recurrent macular edema secondary to central retinal venous occlusion. Indian Journal of Ophthalmology 63, 469–470. [PubMed: 26139820]

Chhablani J, Dedhia CJ, Peguda HK, Stewart M, 2017 SHORT-TERM SAFETY OF 2 MG INTRAVITREAL ZIV-AFLIBERCEPT. RETINA 37, 1859–1865. [PubMed: 28060148]

Constable PA, Lawrenson JG, 2009 Glial cell factors and the outer blood retinal barrier. Ophthalmic and Physiological Optics 29, 557–564. [PubMed: 19689550]

de Oliveira Dias J, Xavier C, Maia A, de Moraes N, Meyer C, Farah M, Rodrigues E, 2015 Intravitreal Injection of Ziv-Aflibercept in Patient With Refractory Age-Related Macular Degeneration. Ophthalmic Surg Lasers Imaging Retina. 46, 91–94. [PubMed: 25559518]

de Oliveira Dias JR, Costa de Andrade G, Kniggendorf VF, Novais EA, Takahashi VKL, Maia A, Meyer C, Watanabe SES, Farah ME, Rodrigues EB, 2017 INTRAVITREAL ZIV-AFLIBERCEPT FOR NEOVASCULAR AGE-RELATED MACULAR DEGENERATION: 52-Week Results. RETINA Publish Ahead of Print.

de Oliveira Dias JR, de Andrade GC, Novais EA, Farah ME, Rodrigues EB, 2016 Fusion proteins for treatment of retinal diseases: aflibercept, ziv-aflibercept, and conbercept. International journal of retina and vitreous 2, 3–3. [PubMed: 27847621]

Deissler HL, Deissler H, Lang GE, 2012 Actions of bevacizumab and ranibizumab on microvascular retinal endothelial cells: similarities and differences. British Journal of Ophthalmology 96, 1023–1028. [PubMed: 22539748]

Do DV, Nguyen QD, Boyer D, Schmidt-Erfurth U, Brown DM, Vitti R, Berliner AJ, Gao B, Zeitz O, Ruckert R, Schmelter T, Sandbrink R, Heier JS, 2012 One-Year Outcomes of the DA VINCI Study of VEGF Trap-Eye in Eyes with Diabetic Macular Edema. Ophthalmology 119, 1658–1665. [PubMed: 22537617]

Do DV, Nguyen QD, Khwaja AA, Channa R, Sepah YJ, Sophie R, Hafiz G, Campochiaro PA, READ-2 Study Group, f.t., 2013 Ranibizumab for Edema of the Macula in Diabetes Study: 3-Year

Outcomes and the Need for Prolonged Frequent TreatmentRanibizumab for Edema of the Macula. JAMA Ophthalmology 131, 139–145. [PubMed: 23544200]

Dunn KC, Aotaki-Keen AE, Putkey FR, Hjelmeland LM, 1996 ARPE-19, A Human Retinal Pigment Epithelial Cell Line with Differentiated Properties. Experimental Eye Research 62, 155–170. [PubMed: 8698076]

Franceschi C, Campisi J, 2014 Chronic inflammation (inflammaging) and its potential contribution to age-associated diseases. The journals of gerontology. Series A, Biological sciences and medical sciences 69 Suppl 1, S4–9.

Franze K, Grosche J, Skatchkov SN, Schinkinger S, Foja C, Schild D, Uckermann O, Travis K, Reichenbach A, Guck J, 2007 Müller cells are living optical fibers in the vertebrate retina. Proceedings of the National Academy of Sciences 104, 8287–8292.

García M, Vecino E, 2003 Role of Müller glia in neuroprotection and regeneration in the retina. Histol Histopathol 18, 1205–1218. [PubMed: 12973689]

Glisic-Milosavljevic S, Waukau J, Jana S, Jailwala P, Rovensky J, Ghosh S, 2005 Comparison of apoptosis and mortality measurements in peripheral blood mononuclear cells (PBMCs) using multiple methods. Cell Proliferation 38, 301–311. [PubMed: 16202038]

Golan S, Entin-Meer M, Semo Y, Maysel-Auslender S, Mezad-Koursh D, Keren G, Loewenstein A, Barak A, 2014 Gene profiling of human VEGF signaling pathways in human endothelial and retinal pigment epithelial cells after anti VEGF treatment. BMC Research Notes 7, 617. [PubMed: 25201034]

Goldberg EL, Dixit VD, 2015 Drivers of age-related inflammation and strategies for healthspan extension. Immunological reviews 265, 63–74. [PubMed: 25879284]

Group, B.P.N.W., 2012 LA. C. Memorandum Addendum - BLA 125418 - Zaltrap ([xxx]-aflibercept) manufactured by sanofi aventis, U.S, LLC..

Grunwald JE, Daniel E, Huang J, Ying G. s., Maguire MG, Toth CA, Jaffe GJ, Fine SL, Blodi B, Klein ML, Martin AA, Hagstrom SA, Martin DF, 2014 Risk of Geographic Atrophy in the Comparison of Age-related Macular Degeneration Treatments Trials. Ophthalmology 121, 150–161. [PubMed: 24084496]

Guo B, Wang Y, Hui Y, Yang X, Fan Q, 2010 Effects of anti-VEGF agents on rat retinal Müller glial cells. Molecular vision 16, 793–799. [PubMed: 20454698]

Hollborn M, Ulbricht E, Rillich K, Dukic-Stefanovic S, Wurm A, Wagner L, Reichenbach A, Wiedemann P, Limb GA, Bringmann A, Kohen L, 2011 The human Muller cell line MIO-M1 expresses opsins. Mol Vis 17, 2738–2750. [PubMed: 22065927]

Idziorek T, Estaquier J, De Bels F, Ameisen J-C, 1995 YOPRO-1 permits cytofluorometric analysis of programmed cell death (apoptosis) without interfering with cell viability. Journal of Immunological Methods 185, 249–258. [PubMed: 7561136]

Klettner A, Möhle F, Roider J, 2010 Intracellular bevacizumab reduces phagocytotic uptake in RPE cells. Graefe's Archive for Clinical and Experimental Ophthalmology 248, 819–824.

Limb GA, Salt TE, Munro PMG, Moss SE, Khaw PT, 2002 In Vitro Characterization of a Spontaneously Immortalized Human Müller Cell Line (MIO-M1). Investigative ophthalmology & visual science 43, 864–869. [PubMed: 11867609]

Luthra S, Narayanan R, Marques LE, Chwa M, Kim DW, Dong J, Seigel GM, Neekhra A, Gramajo AL, Brown DJ, Kenney MC, Kuppermann BD, 2006 Evaluation of in vitro effects of bevacizumab (Avastin) on retinal pigment epithelial, neurosensory retinal, and microvascular endothelial cells. Retina 26, 512–518. [PubMed: 16770256]

Malik D, del Carpio JC, Kim YG, Moustafa MTM, Thaker K, Patel T, Bababeygy SR, Kenney CM, Kuppermann B, 2014a Mitochondrial Membrane Potential Response of Retinal Pigment Epithelium Cells In Vitro to Anti-VEGF Agents: Ranibizumab, Bevacizumab, Aflibercept and Ziv-aflibercept. Investigative ophthalmology & visual science 55, 599–599.

Malik D, Tarek M, Caceres del Carpio J, Ramirez C, Boyer D, Kenney MC, Kuppermann BD, 2014b Safety profiles of anti-VEGF drugs: bevacizumab, ranibizumab, aflibercept and ziv-aflibercept on human retinal pigment epithelium cells in culture. British Journal of Ophthalmology 98, i11–i16. [PubMed: 24836865]

Manousaridis K, Talks J, 2012 Macular ischaemia: a contraindication for anti-VEGF treatment in retinal vascular disease? British Journal of Ophthalmology 96, 179–184. [PubMed: 22250209]

Mansour AM, Al-Ghadban SI, Yunis MH, El-Sabban ME, 2015 Ziv-aflibercept in macular disease. British Journal of Ophthalmology 99, 1055–1059. [PubMed: 25677668]

Mansour AM, Ashraf M, Dedhia CJ, Charbaji A, Souka AAR, Chhablani J, 2017a Long-term safety and efficacy of ziv-aflibercept in retinal diseases. British Journal of Ophthalmology 101, 1374–1376. [PubMed: 28270485]

Mansour AM, Dedhia C, Chhablani J, 2017b Three-month outcome of intravitreal ziv-aflibercept in eyes with diabetic macular oedema. British Journal of Ophthalmology 101, 166–169. [PubMed: 27190127]

Martin DF, Maguire MG, Fine SL, Ying G. s., Jaffe GJ, Grunwald JE, Toth C, Redford M, Ferris FL, 2012 Ranibizumab and Bevacizumab for Treatment of Neovascular Age-related Macular Degeneration: Two-Year Results. Ophthalmology 119, 1388–1398. [PubMed: 22555112]

Matsuda M, Krempel PG, Marquezini MV, Sholl-Franco A, Lameu A, Monteiro MLR, Miguel N.C.d.O., 2017 Cellular stress response in human Müller cells (MIO-M1) after bevacizumab treatment. Experimental Eye Research 160, 1–10. [PubMed: 28419863]

Matsuzaki K, Tomioka M, Watabe Y, 2014 Expression of the Sortilin Gene in Cultured Human Keratinocytes Increases in a Glucose-free Medium. Clinical Research on Foot & Ankle, 1–5.

Mosmann T, 1983 Rapid colorimetric assay for cellular growth and survival: Application to proliferation and cytotoxicity assays. Journal of Immunological Methods 65, 55–63. [PubMed: 6606682]

Ozawa Y, Toda E, Kawashima H, Homma K, Osada H, Nagai N, Abe Y, Yasui M, Tsubota K, 2019 Aquaporin 4 Suppresses Neural Hyperactivity and Synaptic Fatigue and Fine-Tunes Neurotransmission to Regulate Visual Function in the Mouse Retina. Mol Neurobiol 12, 019–01661.

Pereiro X, Ruzafa N, Acera A, Fonollosa A, Rodriguez FD, Vecino E, 2018 Dexamethasone protects retinal ganglion cells but not Muller glia against hyperglycemia in vitro. PloS one 13.

Ramírez C, Cáceres-del-Carpio J, Chu J, Chu J, Moustafa MT, Chwa M, Limb GA, Kuppermann BD, Kenney MC, 2016 Brimonidine can prevent in vitro hydroquinone damage on retinal pigment epithelium cells and retinal Müller cells. Journal of Ocular Pharmacology and Therapeutics 32, 102–108. [PubMed: 26624556]

Reichenbach A, Bringmann A, 2013 New functions of Müller cells. Glia 61, 651–678. [PubMed: 23440929]

Rios MN, Marchese NA, Guido ME, 2019 Expression of Non-visual Opsins Opn3 and Opn5 in the Developing Inner Retinal Cells of Birds. Light-Responses in Muller Glial Cells. Front Cell Neurosci 13.

Romano MR, Biagioni F, Besozzi G, Carrizzo A, Vecchione C, Fornai F, Lograno MD, 2012 Effects of bevacizumab on neuronal viability of retinal ganglion cells in rats. Brain research 1478, 55–63. [PubMed: 23046588]

Rosenfeld PJ, Brown DM, Heier JS, Boyer DS, Kaiser PK, Chung CY, Kim RY, 2006 Ranibizumab for Neovascular Age-Related Macular Degeneration. New England Journal of Medicine 355, 1419–1431. [PubMed: 17021318]

Sarthy P, Lam D, 1978 Biochemical studies of isolated glial (muller) cells from the turtle retina. The Journal of Cell Biology 78, 675–684. [PubMed: 29902]

Schnichels S, Hagemann U, Januschowski K, Hofmann J, Bartz-Schmidt K-U, Szurman P, Spitzer MS, Aisenbrey S, 2013 Comparative toxicity and proliferation testing of aflibercept, bevacizumab and ranibizumab on different ocular cells. British Journal of Ophthalmology 97, 917–923. [PubMed: 23686000]

Singh SR, Dogra A, Stewart M, Das T, Chhablani J, 2017 Intravitreal Ziv-Aflibercept: Clinical Effects and Economic Impact. Asia Pac J Ophthalmol 6, 561–568.

Spitzer MS, Yoeruek E, Sierra A, Wallenfels-Thilo B, Schraermeyer U, Spitzer B, Bartz-Schmidt KU, Szurman P, 2007 Comparative antiproliferative and cytotoxic profile of bevacizumab (Avastin), pegaptanib (Macugen) and ranibizumab (Lucentis) on different ocular cells. Graefe's Archive for Clinical and Experimental Ophthalmology 245, 1837–1842.

TDRCR N, 2015 Aflibercept, Bevacizumab, or Ranibizumab for Diabetic Macular Edema. New England Journal of Medicine 372, 1193–1203. [PubMed: 25692915]

Tian J, Ishibashi K, Honda S, Boylan SA, Hjelmeland LM, Handa JT, 2005 The expression of native and cultured human retinal pigment epithelial cells grown in different culture conditions. The British journal of ophthalmology 89, 1510–1517. [PubMed: 16234463]

Tufail A, Patel PJ, Egan C, Hykin P, da Cruz L, Gregor Z, Dowler J, Majid MA, Bailey C, Mohamed Q, Johnston R, Bunce C, Xing W, 2010 Bevacizumab for neovascular age related macular degeneration (ABC Trial): multicentre randomised double masked study. BMJ 340, c2459. [PubMed: 20538634]

Wu PC, Chen YJ, Chen CH, Chen YH, Shin SJ, Yang HJ, Kuo HK, 2008 Assessment of macular retinal thickness and volume in normal eyes and highly myopic eyes with third-generation optical coherence tomography. Eye (Lond) 22, 551–555. [PubMed: 17464309]

Zehetner C, Bechrakis NE, Stattin M, Kirchmair R, Ulmer H, Kralinger MT, Kieselbach GF, 2015 Systemic Counterregulatory Response of Placental Growth Factor Levels to Intravitreal Aflibercept TherapySystemic PlGF Upregulation After Intravitreal Aflibercept. Investigative ophthalmology & visual science 56, 3279–3286. [PubMed: 26024110]

HIGHLIGHTS

- Human retinal Müller cells (MIO-M1) were treated with 4 different anti-VEGF drugs.
- Cultures had decreased metabolism, viability and mitochondrial membrane potential.
- Treatment led to higher levels of ROS and apoptosis.
- Altered expression of angiogenesis, pro-apoptosis and inflammatory genes were found.
- Anti-VEGF drugs may contribute to cytotoxicity associated with chronic injections.

Cáceres-del-Carpio Table 1:

Gene symbol, name, gene bank accession number and function.

Gene Symbol *	Gene Name†	Gene Bank Accession Num.‡	Function§
GPX3	Glutathione peroxidase 3	NM_002084	Catalyzes the reduction of hydrogen peroxide.
SOD2	Superoxide dismutase 2, mitochondria	NM_000636 NM_001024465	Converts the superoxide byproducts to H_2O_2 and O_2.
IL1β	Interleukin 1, beta (also known as IL-1β)	NM_000576, XM_006712496	Encodes a cytokine involving cell proliferation, differentiation and apoptosis.
IL18	Interleukin 18	NM_001243211 NM_001562	Cytokine that stimulates natural killer cell activity and interferon gamma production.
BCL2L13	BCL2-like 13 (apoptosis facilitator)	NM_015367	Encodes a mitochondrial-localized protein. Overexpression results in apoptosis.
BAX	BCL2-associated X protein (also known as BCL2L4)	NM_004324, NM_138761, NM_138763, NM_138764, NM_138765, NR_027882, NM_001291428, NM_001291429, NM_001291430, NM_001291431, XM_006723314	Encodes a pro-apoptotic protein.
VEGFA	Vascular endothelial growth factor A	NM_001025366, NM_001025367, NM_001025368, NM_001033756, NM_001171623, NM_001171624, NM_001171625, NM_001171626, NM_001171629, NM_003376, NM_001287044	Encodes a protein that induces angiogenesis, vasculogenesis and inhibition of apoptosis.
PGF	Placental growth factor (also known as PLGF)	NM_001207012, NM_002632, NM_001293643	Encodes a growth factor homologous to vascular endothelial growth factor.
HIF1A	Hypoxia inducible factor 1 alpha	NM_001243084, NM_001530, NM_181054	In response to adaptation to hypoxia, activates transcription of genes involved in energy metabolism, angiogenesis, apoptosis and oxygen delivery.

*Official gene symbol by HUGO (Human Genome Organization) Gene Nomenclature Committee (HGNC).

†Official gene name by HUGO Gene Nomenclature Committee (HGNC).

‡Gene Accession Bank Number from the primers used (Qiagen, Valencia, CA).

§Gene function modified from PubMed gene.

Table 2.

Differences in gene expression MIO-M1 cells after treatment with 1x and 2x anti-VEGF drugs 2A. Treated with Ranibizumab. 2B treated with bevacizumab. 2C Treated with aflibercept. 2D Treated with ziv-aflibercept

Table 2A. MIO - MI Treated with ranibizumab

	1x		2x	
Gene	**Fold**	**P**	**Fold**	**P**
VEGFA †	0.66	0.029 *	0.41	0.0008 *
PGF †	1.11	0.55	1.41	0.066
HIF1A †	1.2	0.29	2.26	0.094
BAX ‡	1.06	0.58	0.93	0.56
BCL2L13 ‡	0.91	0.23	1.05	0.55
IL1β §	5.12	0.0001 *	4.58	0.0002 *
IL18 §	1.43	0.0175 *	1.39	0.017 *
GPX3 #	2.31	0.0001 *	1.96	0.0001 *
SOD2 #	0.58	0.002 *	0.3	0.0006 *

Table 2B. MIO-M1 treated with bevacizumab

	1x		2x	
Ge ne	**Fold**	**P**	**Fold**	**P**
VEGFA †	0.65	0.0016 *	0.41	0.0187 *
PGF †	1.79	0.0132 *	1.49	0.036
HIF1A †	1.41	0.35	0.94	0.92
BAX ‡	1.22	0.0114 *	1.01	0.82
BCL2L13 ‡	1.38	0.0015 *	1.6	0.0007 *
IL1β §	1.8	0.0041 *	1.19	0.15
IL18 §	1.57	0.13	1.1	0.73
GPX3 #	2.13	0.0011 *	2.22	0.0006 *
SOD2 #	0.69	0.0402 *	0.41	0.0013 *

Table 2C. MIO-M1 Treated with aflibercept

	1x		2x	
Gene	**Fold**	**P**	**Fold**	**P**
VEGFA †	0.55	0.0037 *	0.58	0.0136 *
PGF †	2.2	0.0147 *	1.84	0.0108 *
HIF1A †	1.48	0.22	1.34	0.26
BAX ‡	0.98	0.75	1.08	0.19
BCL2L13 ‡	1.35	0.0094 *	1.21	0.0132 *

IL1β[§]	1.19	0.2	0.89	0.6
IL18[§]	0.63	0.19	0.95	0.85
GPX3[#]	2.18	0.0002[*]	1.67	0.001[*]
SOD2[#]	0.22	<0.0001[*]	0.44	0.0014[*]

Table 2D. MIO-M1 treated with ziv-Aflibercept

	1x		2x	
Gene	**Fold**	**P**	**Fold**	**P**
VEGFA[†]	0.88	0.014[*]	0.92	0.618
PGF[†]	0.7	0.0245[*]	0.53	0.0063[*]
HIF1A[†]	1.06	0.69	1.09	0.61
BAX[‡]	1.85	0.0009[*]	1.46	0.0005[*]
BCL2L13[‡]	1.04	0.485	1.29	0.053
IL1β[§]	1	0.99	1.21	0.563
IL18[§]	1.96	0.0164[*]	1.88	0.0168[*]
GPX3[#]	0.95	0.457	1.17	0.156
SOD2[#]	0.22	<0.0001[*]	0.24	<0.0001[*]

9 genes were tested, each one was tested 2 times in triplicates.

Fold values > 1 indicates upregulation of the gene compared with untreated control; Fold values < 1 indicates downregulation of the gene compared with untreated control; Control samples assigned a value of 1.

1x: equivalent to the clinical doses of anti-VEGF (0.05ml injected in 4ml of vitreous).

2x: equivalent to double the clinical dose of anti-VEGF.

Folds were calculated with the formula 2ΔΔCt.

[*] $p < 0.05$;

[†] Angiogenesis;

[‡] Pro-apoptosis;

[§] Inflammation;

[#] Oxidative stress.